COMPUTER SIMULATION OF FLAGELLAR MOVEMENT

IV. PROPERTIES OF AN OSCILLATORY TWO-STATE CROSS-BRIDGE MODEL

C. J. BROKAW

From the Division of Biology, California Institute of Technology,
Pasadena, California 91125

ABSTRACT A stochastic computational method is used to examine the properties of a simple two-state cross-bridge model, of a type which has been shown previously to self-oscillate without requiring any feedback control of the active process. The force transients obtained with this model show the major features observed with oscillatory insect fibrillar flight muscle. The effects of viscosity and cross-bridge detachment rate on the frequency of oscillation of the model resemble the effects of viscosity and ATP concentration on flagellar oscillation, and the relationship between turnover rate and frequency of oscillation is also consistent with observations on flagella. However, the amplitude of oscillation of the model does not show the degree of frequency-independence which is typical of flagella.

INTRODUCTION

Oscillatory properties inherent in the specifications of attachment and detachment rates for force-generating cross-bridges have been suggested as a possible mechanism for oscillation in flagella and in insect fibrillar flight muscle (Brokaw, 1975*a*). Examination of the suitability of this oscillatory mechanism for flagella can be carried out by using the method for computer simulation of cross-bridge behavior, developed in the preceding paper, and methods used earlier for computer simulation of flagellar movement (Brokaw, 1972) to examine the behavior of a flagellar model with cross-bridges distributed throughout its length. Since it is anticipated that the expense of computing such models will be sufficient to severely limit the number of computations which can be performed, this approach needs to be preceded by a careful comparison of the oscillatory properties of cross-bridge models with the experimentally observed properties of flagellar oscillation. In the present paper, the properties of a two-state cross-bridge model with oscillatory properties, similar to the model described briefly by Brokaw (1975*a*), are examined in detail, using the stochastic computational method developed in the preceding paper (Brokaw, 1976).

SPECIFICATIONS FOR AN OSCILLATORY TWO-STATE CROSS-BRIDGE MODEL

This model uses rate and force functions of the same form as those used for the modified two-state model in the preceding paper, with the attachment rate function, $f(x)$, based on the idea that rotation of an unattached cross-bridge around its base is responsible for the variation in attachment probability with position. Some of the numerical parameters have been modified to give the model properties similar to those of the previously described oscillatory model (Brokaw, 1975*a*). The rate functions are illustrated in the inset in Fig. 1. The attachment rate function is much narrower, and is given by

$$f(x) = 180\exp(-64\theta^2)\ \mathrm{s}^{-1}, \tag{1}$$

with θ defined by equation 20 in the preceding paper (Brokaw, 1976). The detachment rate function, $g(x)$ is given by

$$g(x) = G + 1.5G\exp(-0.35x). \tag{2}$$

The constant G was given a value of 10 s^{-1}. The cross-bridge force constant, k_F, is given a higher value, 1.6 pN nm^{-1}, which locates the steep rise of the reverse attachment rate function, $f'(x)$, near the midpoint of the peak of the $f(x)$ curve. Other

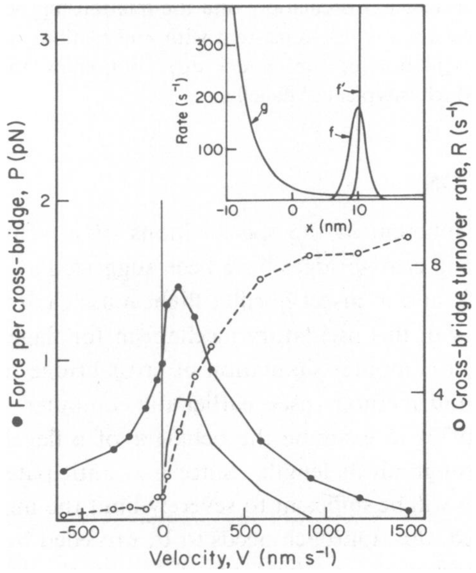

FIGURE 1 Steady-state behavior of the oscillatory cross-bridge model, with rate functions illustrated in the inset. Computed with 800 cross-bridges, and $dt = 0.001$ s, with the points representing a time average over the last 0.15 s of a 0.3 s computation at each velocity. The lower curve, without points, represents the net force for a pair of antagonistic cross-bridge systems, obtained from $P(V) - P(-V)$.

parameters are identical to those used for the modified two-state model in the preceding paper.

RESULTS

Force at Constant Velocity

The results obtained from stochastic computations of the behavior of the oscillatory cross-bridge model during steady shortening and stretching are shown in Fig. 1. The specifications for the model were chosen to keep V_{max} near 1600 nm s^{-1} and R_{max} near 8 s^{-1}, as obtained with the two models in the previous paper, while enhancing the property that the force which resists stretching, $P(-V)$, is much less than $P(V)$, the force generated during shortening. The lower curve in Fig. 1 shows the net force, $P(V) - P(-V)$ for an antagonistic pair of identical cross-bridge populations with these properties. The velocity for 0 force for the pair of cross-bridge populations is reduced to about 900 nm s^{-1}. The maximum work output per cross-bridge cycle for the antagonistic pair of cross-bridge populations is approximately 30 pN nm, corresponding to an energy efficiency of 30% if the energy input per ATP molecule, ΔkT, is 100 pN nm. For comparison, the Huxley model considered in the previous paper gives a maximum efficiency of 39% with the same assumptions.

The efficiency of the oscillatory model considered here is somewhat less than that of the one considered originally (Brokaw, 1975*a*), which had somewhat more arbitrary rate functions.

Force Transients

Responses of a single one of these cross-bridge systems to quick releases and quick stretches of 3 nm are shown in Fig. 2A. These transient responses are quite unlike those shown for the cross-bridge models in the preceding paper, but are easily interpreted by reference to the rate functions depicted in Fig. 1 (insert). After a quick release there is a rapid drop in the force generated by the originally attached cross-bridges, as a result of their simple elastic behavior. A new group of cross-bridges, of comparable number, has moved to positions where they can attach, with a relatively

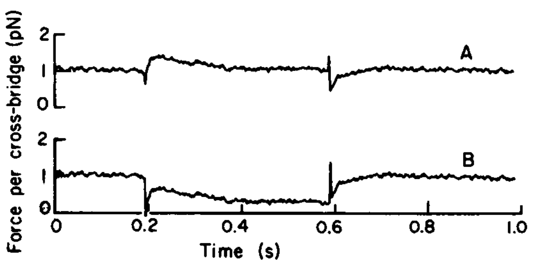

FIGURE 2 Force transients following a quick release of 3 nm and a quick stretch of 3 nm, computed with 1600 cross-bridges and $dt = 0.002$ s. In A, no elastic shear resistance is added to the model. In B, an elastic shear resistance of 0.24 pN nm^{-1} per cross-bridge is added to the model to facilitate comparison with force transients of insect fibrillar muscle.

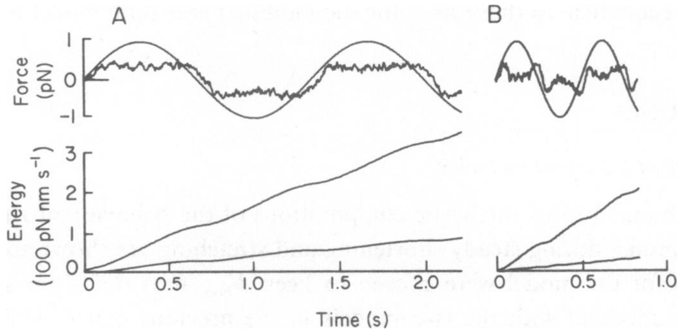

FIGURE 3 Computations with sinusoidally driven oscillation using an antagonistic pair of cross-bridge systems, with 800 cross-bridges in each system. In A, the oscillation frequency was 0.75 Hz, with $dt = 0.004$ s. In B, the oscillation frequency was 2.0 Hz, with $dt = 0.003$ s. Force, $P(t)$, is shown by the irregular curve in the upper part of the diagrams. The smooth sinusoidal curve shows the time variation of shear velocity, but the amplitude of this curve has been arbitrarily set at 1.0 in both cases, as only phase information was needed. In the lower part of the diagrams, the upper curve shows the energy input, equal to the cross-bridge turnover number, and the lower curve shows the work output, as functions of time.

high rate, determined by $f(x)$. This causes a rapid increase in force. There is a slower fall in force, as the originally attached cross-bridges, which have not been carried into a region of high detachment rate, detach at a rate determined by $g(x)$. After a quick stretch, there is an initial force increase resulting from the elastic behavior of the originally attached cross-bridges. These cross-bridges then detach very rapidly, since they have been carried into regions where $f'(x)$ is very high. This is followed by a recovery of force, as a new group of cross-bridges attaches with rate determined by $f(x)$. Since $f'(x)$ and $f(x)$ are larger than $f(x)$ and $g(x)$, respectively, the responses following a stretch will be faster than the responses following a release.

In Fig. 2B, the same transient responses are shown superimposed on a parallel elastic resistance of 0.24 pN nm^{-1} per cross-bridge, to facilitate comparison with force transients obtained from insect fibrillar flight muscle.

Sinusoidally Driven Oscillation

Information about the oscillatory properties of a cross-bridge population can be obtained by imposing sinusoidal changes in shear, $\sigma(t)$, equivalent to a sinusoidally varying velocity, and computing the force $P(t)$ as a function of time. Fig. 3 illustrates results from this type of computation, using two antagonistic cross-bridge populations, each containing 800 cross-bridges. The system was driven with an amplitude of ± 40 nm, which is similar to the amount of sliding between tubules which occurs during flagellar oscillation (Brokaw, 1975*b*). Average force per cross-bridge is shown as a function of time, for two different frequencies of oscillation. A frequency of 0.75 Hz, which gives a peak shear velocity of 188 nm s^{-1}, was used for Fig. 3A, and a frequency of 2.0 Hz, which gives a peak shear velocity of 503 nm s^{-1}, was used for Fig. 3B. The cross-bridge turnover rate and the power (equal to the product of the imposed

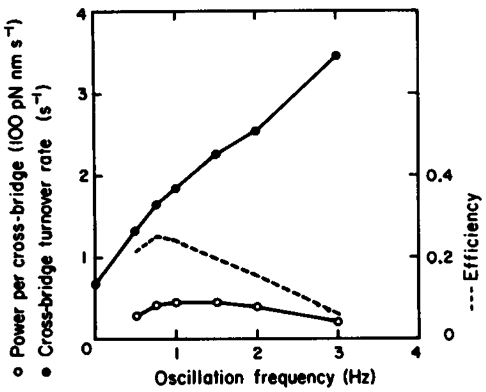

FIGURE 4 Summary of energy input and output during sinusoidally driven oscillations at various frequencies, obtained from computations like those shown in Fig. 3. The efficiency is based on the assumption that cross-bridge turnover rate represents the rate at which energy is provided by ATP, at 100 pN nm per molecule of ATP.

velocity and the computed force) were computed and integrated over 1 cycle to obtain average rates of cross-bridge turnover and power output. These are summarized in Fig. 4 for several frequencies in the range of 0.5 to 3 Hz.

At a frequency of 0.75 Hz, which gives nearly maximal efficiency, a fairly constant force, in the direction of sliding, is generated during sliding in each direction. At higher frequencies, as shown in Fig. 3B, the force is reduced during the portions of the cycle having the highest velocities, as might be expected from the force-velocity behavior (Fig. 1), and the efficiency is reduced. At both frequencies, the force lags slightly behind the sinusoidal variation in velocity, as a result of the kinetics of adjustment of the cross-bridge population to changes in length. This delay might limit the efficiency of the system during small amplitude oscillation at high frequencies, but with the amplitude used for these computations, the velocity limitation is much more significant than the time lag limitation. Since the time lag effects are small, a reasonable estimate of the behavior during sinusoidally driven oscillation could be obtained from computations of the steady-state force-velocity relationship (Fig. 1).

Free Oscillation

Addition to the antagonistic pair of cross-bridge systems of an elastic shear resistance, E_S, tending to restore the shear, σ, to 0, is sufficient to create a system which will oscillate spontaneously (Brokaw, 1975*a*). Computation of the motion during free oscillation encounters the same problems which arise during computation of isotonic shortening behavior, as described in the preceding paper (Brokaw, 1976). However, the problems are less severe in the context of flagellar oscillations, where the useful work is done against a relatively high viscous load (C_S) which stabilizes the computations. Examples of computations of free oscillation are shown in Fig. 5, at two different viscosities. These computations were carried out using the method used for Fig. 5C of the preceding paper (Brokaw, 1976), with $d\sigma$, the change in shear in a time interval

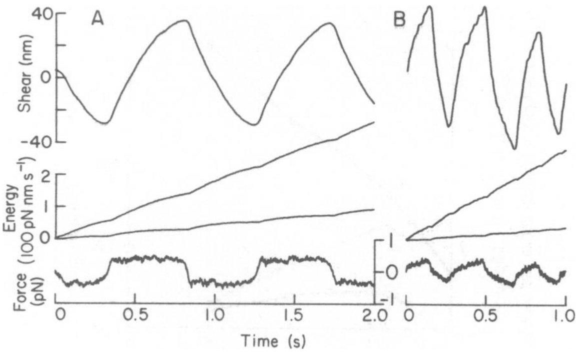

FIGURE 5 Computations of free oscillation of an antagonistic pair of cross-bridge systems, with 800 cross-bridges per system. In A, the shear viscosity, C_S, had a value of 0.002 pN s nm^{-1} per cross-bridge, and $dt = 0.002$ s. In B, $C_S = 0.00025$ pN s nm^{-1} and $dt = 0.001$ s. The upper and lower energy curves show energy input and output, as in Fig. 3.

dt, calculated from

$$d\sigma = [-P(t) - E_S\sigma - 0.5\,k_F N(t) d\sigma + s(t - dt)]\,dt/C_S \qquad (3)$$

where

$$s(t) = 0.05\,k_F N(t) d\sigma + 0.9\,s(t - dt) \qquad (4)$$

and $N(t)$ = the fraction of cross-bridges which are attached at time t. The output from these computations, as shown especially in Fig. 5B, is not completely periodic, and the irregularities become even greater at lower viscosities. Accurate measurement of the oscillation frequency from the output requires that several cycles of oscillation be computed, with a relatively small time step to minimize irregularities. Consequently, even with the correction terms included in equation 3, the cost for computation of the results shown in Fig. 5B is four times that for the results shown in Fig. 3B, using driven oscillations. The free oscillations are clearly nonsinusoidal and have the

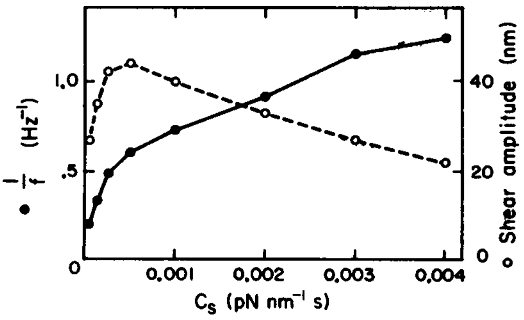

FIGURE 6 Amplitude and frequency for free oscillations of the cross-bridge model, with E_S = 0.008 pN nm^{-1} per cross-bridge, at various values of C_S, obtained from computations like those shown in Fig. 5.

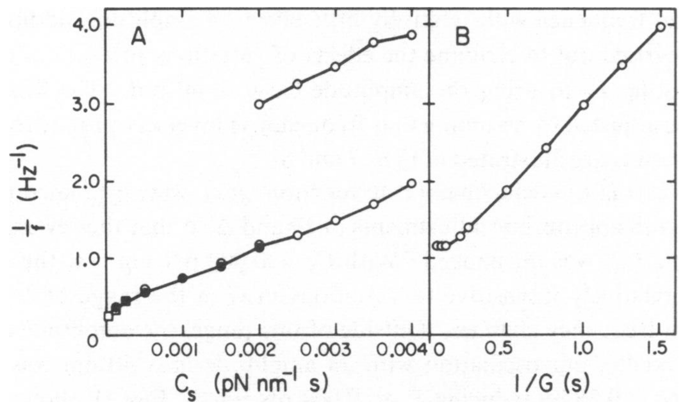

FIGURE 7 Frequency for free oscillations of the cross-bridge model with E_S adjusted to obtain the frequency at an amplitude of 40 nm. For the lower curve in Fig. 7A, $G = 10$ s^{-1}, the open circles show results obtained with $dt = 0.002$ s, the solid circles show results obtained with $dt = 0.001$ s, and the open squares show results obtained with $dt = 0.0005$ s. For the upper curve in Fig. 7A, $G = 1$ s^{-1}, and $dt = 0.005$ s. Values of dt used for Fig. 7B ranged from 0.002 to 0.006 s, with $C_S = 0.002$ pN nm^{-1} s.

character of typical relaxation oscillations, as described previously (Brokaw, 1975*a*). Consequently, the $P(t)$ curve is quite different from that for sinusoidal oscillations, at the higher frequencies, and does not show the dip in force in the midregion of the wave. The efficiency appears to be slightly higher during free oscillation than during sinusoidally driven oscillation.

Fig. 6 summarizes frequency and amplitude values obtained from computations of this type at various values of C_S, all with $E_S = 0.008$ pN nm^{-1} per cross-bridge. Both amplitude and frequency change substantially with viscosity. In order to facilitate comparison with observations on sperm flagella where viscosity changes cause

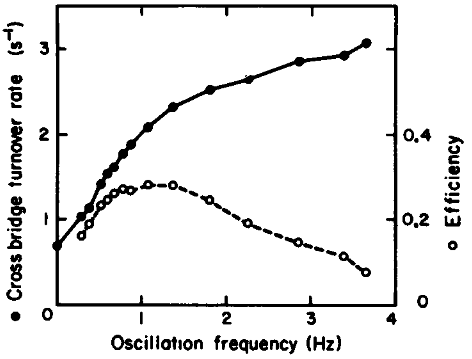

FIGURE 8 Summary of energy input and efficiency for free oscillations at various frequencies, from the computations corresponding to the lower curve in Fig. 7A. The efficiency is based on the assumption that cross-bridge turnover rate represents the rate at which energy is provided by ATP, at 100 pN nm per molecule of ATP.

changes in beat frequency with relatively little effect on amplitude, additional computations were carried out to examine the effects of variations in C_S at constant amplitude, by adjusting E_S to bring the amplitude close to 40 nm. The final estimate of frequency was adjusted by assuming that frequency is inversely proportional to amplitude. These results are illustrated in Figs. 7 and 8.

Effects of varying the detachment rate function, $g(x)$, were examined by varying G [equation 2], with appropriate adjustments in Γ' and Δ so that the reverse detachment rate function, $g'(x)$, was unchanged. With $C_S = 0.002$ pN nm^{-1} s, the amplitude of oscillation is relatively insensitive to variations in G in the range of 1–10 s^{-1}, while the oscillation frequency changes. Outside of this range, the amplitude of oscillation decreases markedly, but oscillation with an amplitude near 40 nm was obtained at $G = 20$ and $G = 0.25$ by reducing E_S to 0.004 pN nm^{-1}. Fig. 7B shows the relationship between oscillation frequency, adjusted to an amplitude of 40 nm, and G, as a double reciprocal plot, which can be compared with that found when flagellar beat frequency is plotted against ATP concentration (Brokaw, 1967, 1975*c*). The oscillation frequency obtained when C_S is varied at $G = 1$ s^{-1} is also shown by the upper curve in Fig. 7A.

DISCUSSION

The self-oscillatory behavior of the type of cross-bridge system examined in this paper has been explained previously in terms of the steady-state behavior of the antagonistic pair of cross-bridge systems (Brokaw, 1975*a*), with each system generating greater force during shortening than during stretching. The behavior required for oscillation is also demonstrated during sinusoidally driven oscillations and by the force transients following suddenly applied length changes, which show a delayed increase in force following stretch, and a delayed decrease in force following release (Fig. 2). The steady-state tension of self-oscillatory insect fibrillar muscle shows an additional length dependence which may be functionally equivalent to the shear elasticity, E_S, which must be added to the cross-bridge systems in order to obtain self-oscillation. When an appropriate shear elasticity is included, force transient behavior of the oscillatory cross-bridge system, as shown in Fig. 2B, is basically similar to the force transient behavior observed with insect fibrillar muscle (Jewell and Ruegg, 1966; Tregear, 1975). However, the force transient response of insect fibrillar muscle is symmetrical, with identical time constants for the force transients following release and following stretch. There is no obvious way to modify the specification of this two-state cross-bridge model to give symmetrical force transient behavior.

A feedback control of cross-bridge interactions by stretch has been suggested previously as a basis for oscillation in insect fibrillar muscle (Pringle, 1967; Thorson and White, 1969; Julian, 1969). Similarly, a feedback control of cross-bridge interactions by curvature has been suggested as a basis for oscillation and bend propagation by flagella (Brokaw, 1971, 1972; Brokaw and Rintala, 1975). The self-oscillatory cross-bridge model considered here offers an alternative basis for oscillation both for insect fibrillar muscle and for flagella. In both cases, further work appears to be required to determine the actual mechanism for oscillation. Since the amplitudes of normal operation for a cross-bridge system in flagella are an order of magnitude larger than in insect fibrillar muscle, some properties of the two systems may be different even if both use the same mechanism for oscillation. For example, the value of E_S used for Fig. 2B to obtain transient responses similar to insect fibrillar muscle would be appropriate for oscillatory amplitudes closer to 2 nm, rather than the 40 nm amplitudes of interest for flagella.

When an undulatory bending wave, such as a sine-generated wave, is propagated along a flagellum, the maximum active shear moment to overcome viscous resistances is required at the crests of the wave, in the same regions where the velocity of sliding between tubules is maximum (Goldstein, 1976). This correspondence is contrary to the typical force-velocity relationship observed with muscle, which shows an inverse relationship between force and velocity. This problem is clearly illustrated in Fig. 3B, where the force generated by a cross-bridge system during sinusoidally driven oscillation decreases during the maximum-velocity portions of the oscillatory cycle. These considerations suggest that the type of cross-bridge model developed for muscle might be inappropriate for flagella. However, the computations with the cross-bridge model considered in this paper indicate that this problem can be avoided if the frequency of oscillation is kept low enough so that the pattern of force generation resembles that in Figs. 3A or 5A. At these lower frequencies of oscillation, which correspond to the range of maximum efficiency for the system, the system operates near the peak of the $P(V)$ relationship for an antagonistic pair of systems, shown by the lower solid curve in Fig. 1, where the changes in P with V are relatively small. With a flagellum operating in this range, it would be expected that changes in frequency, and shear velocity, caused by changes in viscosity might be associated with relatively small changes in calculated shear moment. In fact, this is just what has been observed (Brokaw, 1966, 1975 *b*) for spermatozoa of a sea urchin (*Lytechinus*) and a tunicate (*Ciona*), although not for spermatozoa of an annelid worm (*Chaetopterus*) which respond to increased viscosities in a quite different manner.

The effects of viscosity on free oscillation of the model cross-bridge system can be compared with experimental observations on the effects of viscosity on flagellar oscillation. However, changes in viscosity, η, of the fluid environment in which a flagellum is oscillating are not equivalent to changes in shear viscosity, C_S, when the wavelength of the flagellar motion changes with viscosity. The substantial decreases in wavelength which occur when the viscosity, η, is increased (Brokaw, 1966, 1975 *c*) cause the effective C_S to increase much less rapidly than η, so that rather large changes in η, 10-fold or more, are required to obtain two- to threefold reductions in beat frequency. Since experimental data for reactivated sea urchin sperm flagella were found to give straight lines when $1/f$ was plotted against $\eta^{+0.31}$ (Brokaw, 1975 *c*), the frequency data obtained for the model cross-bridge system are shown as plots of $1/f$ vs. C_S in Figs. 6 and 7A.

With live spermatozoa of *Lytechinus* and *Ciona*, both the bend angle and the frequency of flagellar oscillation decrease as the viscosity is increased (Brokaw, 1966, 1975 *c*; Brokaw and Benedict, 1976). The model cross-bridge system shows similar behavior in the C_S range of 0.0005 to 0.004 pN nm^{-1} s (Fig. 6), where the efficiency remains above 20%.

With live spermatozoa of *Chaetopterus*, the decrease in frequency at increased viscosity is accompanied by an increase in bend angle (Brokaw, 1966; Brokaw and Benedict, 1976). The model cross-bridge system shows similar behavior at C_S values below 0.00025 pN nm^{-1} s, but the efficiencies in this range decrease to values below 10%, while the efficiency of *Chaetopterus* spermatozoa appears to be comparable to that of other spermatozoa (Brokaw and Gibbons, 1975; Brokaw and Benedict, 1976).

With ATP-reactivated spermatozoa of *Lytechinus*, relatively constant bend angles are maintained when the frequency is decreased by increased viscosity (Brokaw, 1975 *c*). The region in which nearly constant bend angles are maintained might correspond to the region near the apex of the amplitude-viscosity curve in Fig. 6, or there may be some other mechanism which maintains constant bend angle when the frequency of oscillation changes (Brokaw and Josslin, 1973; Brokaw, 1975 *c*; Brokaw and Gibbons, 1975). The more extensive computations giving the results in Figs. 7 and 8 were carried out with a constant amplitude near 40 nm, to facilitate comparison with the data from ATP-reactivated spermatozoa. These results show a nearly linear relationship between $1/f$ and C_S covering a fourfold range of frequencies. The slope of this line, measured by the change in $1/f$ for a twofold change in C_S, corresponds most closely to the experimental results with ATP-reactivated spermatozoa in the high-viscosity end of the viscosity range (C_S = 0.002–0.004 pN nm^{-1} s). In this range, there is a nearly linear relationship between cross-bridge turnover rate and beat frequency (Fig. 8), in agreement with experimental measurements of the rate of ATP dephosphorylation as a function of viscosity (Brokaw and Benedict, 1968 *a*, *b*; Gibbons and Gibbons, 1972). The turnover rate at 0 frequency (0.68 s^{-1}) and the slope (1.3 ATP per cycle) shown in Fig. 8 depend on the numerical values and functions chosen for the attachment and detachment rate functions, which could be adjusted so that the model would closely match the experimental results. There is nothing in this model which would predict an integral number for the ATP turnover per beat cycle.

For the present model, values of cross-bridge spacing, d_L, and attachment site spacing, d_S, of 42.9 nm and 37.5 nm, respectively, have been carried over from the preceding paper in which cross-bridge behavior for muscle was emphasized. For flagella, it might be expected that both spacings would be related to the 8 nm periodicity of microtubule subunits (Amos and Klug, 1974). Computations were also carried out with models having d_L = 24 nm and d_S = 8.02 nm. With the models, it is necessary to avoid the situation in which d_L is an exact multiple of d_S, but this restriction may be unimportant in real flagella which will not have completely straight and inextensible tubules. With these computations, using a much smaller value for d_S, the increase in turnover rate, R, with shortening velocity, V, was much more rapid at low velocities, so that the behavior during sinusoidally driven oscillations did not show as satisfactory a relationship between turnover rate and frequency of oscillation.

Reactivated sperm flagella show a large dependence of oscillation frequency on ATP concentration, with relatively little change in amplitude. In order to match this behavior, the oscillatory frequency of the model at constant amplitude should obey the equation:

$$1/f = c_1 C_S + c_2/C, \tag{5}$$

which is modified from equation 2 of Brokaw (1975 *c*) with C_S representing the effective viscosity. C is the ATP concentration and c_1 and c_2 are constants. At constant ATP concentration, this equation accurately describes the frequency-viscosity behavior of the model, as shown in Fig. 7A. The computations carried out using $\Delta kT = 100$ pN nm (14.4 kcal/mole) for the free energy input per ATP molecule ought to correspond to the situation of very high ATP concentration, where the last term in equation 5 is very small. If the $1/f$ intercept at 0 C_S is not 0, a more accurate equation would include another constant, c_3:

$$1/f = c_1 C_S + c_2/C + c_3, \tag{6}$$

as a description of the desired behavior of the model.

Since reductions in ATP concentration cause flagella to enter a rigor state (Gibbons and Gibbons, 1974), the effect of ATP concentration on the oscillatory cross-bridge model could be incorporated by making one of the detachment rate functions, $f'(x)$ or $g(x)$, proportional to C. Any severe change in $f'(x)$ will completely alter the oscillatory properties of the model, so that having $f'(x)$ proportional to C would be inconsistent with regular oscillation over a wide range of ATP concentrations. If $g(x)$ is proportional to ATP concentration, the constant G in equation 2 can be treated as C in equation 6. The double-reciprocal plot of frequency and G, shown in Fig. 7B, shows a linear relationship over much of the range of G, in agreement with equation 6. The results diverge from a linear relationship for large values of G (greater than 5 s^{-1}), so that the model does not show the exact Michaelis-Menten behavior deduced from the experimental data and expressed in equation 6. However, for values of G outside the range of 1 to 10 s^{-1}, this comparison depends strongly on the adjustment to constant amplitude. A more valid comparison with the experimental data would require adjustment to the amplitude measured experimentally at a particular ATP concentration, but the amplitude data necessary for this adjustment are not available. The upper curve in Fig. 7A shows that at lower values of G, variations in C_S have less effect on the frequency of oscillation of the model, in agreement with observations of the effect of viscosity on the frequency of flagellar oscillation at reduced ATP concentrations (Brokaw, 1975 *c*). Since the results obtained at $G = 1\ s^{-1}$ and $G = 10\ s^{-1}$ (Fig. 7A) fall on nearly parallel lines, the constant c_1 in equation 6 is independent of G. This model therefore shows the separation of viscosity-dependent and ATP-dependent terms implicit in equation 6, in agreement with the experimental observations expressed in Fig. 9 of Brokaw (1975 *c*), even though the form of the ATP-dependence may not match the experimental data exactly.

The results obtained from computations with this oscillatory cross-bridge model suggest that it may provide a valid explanation for flagellar oscillation as an alternative to the earlier proposal that flagellar oscillation results from a feedback control of the active sliding process by curvature (Brokaw, 1971). However, in its present form the model does not fully explain the situations in which the frequency of flagellar oscillation can be altered without changing the amplitude (Brokaw and Josslin, 1973; Brokaw, 1975 *c*) and in which the amplitude can be altered without changing the frequency (Brokaw and Simonick, 1976). These observations either imply the presence of additional mechanisms which control frequency and/or amplitude, or a different mechanism for oscillation which might not be expected to be sensitive to amplitude.

This work has been supported by a National Institutes of Health grant (GM 21931).

Received for publication 1 March 1976.

REFERENCES

AMOS, L. A., and A. KLUG. 1974. Arrangement of subunits in flagellar microtubules. *J. Cell Sci.* **14**:523.

BROKAW, C. J. 1966. Effects of increased viscosity on the movements of some invertebrate spermatozoa. *J. Exp. Biol.* **45**:113.

BROKAW, C. J. 1967. Adenosine triphosphate usage by flagella. *Science (Wash. D.C.).* **156**:76.

BROKAW, C. J. 1971. Bend propagation by a sliding filament model for flagella. *J. Exp. Biol.* **55**:289.

BROKAW, C. J. 1972. Computer simulation of flagellar movement. I. Demonstration of stable bend propagation and bend initiation by the sliding filament model. *Biophys. J.* **12**:564.

BROKAW, C. J. 1975 *a*. Molecular mechanism for oscillation in flagella and muscle. *Proc. Nat. Acad. Sci. U.S.A.* **72**:3102.

BROKAW, C. J. 1975 *b*. Cross-bridge behavior in a sliding filament model for flagella. *In* Molecules and Cell Movement. S. Inoue and R. E. Stephens, editors. Raven Press, New York. p. 165.

BROKAW, C. J. 1975 *c*. Effects of viscosity and ATP concentration on the movement of reactivated sea-urchin sperm flagella. *J. Exp. Biol.* **62**:701.

BROKAW, C. J. 1976. Computer simulation of movement-generating cross-bridges. *Biophys. J.* **16**:1013.

BROKAW, C. J., and B. BENEDICT. 1968 *a*. Mechanochemical coupling in flagella. I. Movement-dependent dephosphorylation of ATP by glycerinated spermatozoa. *Arch. Biochem. Biophys.* **125**:770.

BROKAW, C. J., and B. BENEDICT. 1968 *b*. Mechanochemical coupling in flagella. II. Effects of viscosity and thiourea on metabolism and motility of *Ciona* spermatozoa. *J. Gen. Physiol.* **52**:283.

BROKAW, C. J., and B. BENEDICT. 1976. Mechanochemical coupling in flagella. IV. Absence of coupling between metabolism and motility in *Chaetopterus* spermatozoa. *J. Mechanochem. Cell Motility.* **3**:201.

BROKAW, C. J., and I. R. GIBBONS. 1975. Mechanisms of movement in flagella and cilia. *In* Swimming and Flying in Nature. Vol. 1 T. Y.-T Wu, C. J. Brokaw, and C. Brennen. editors. Plenum Publishing Corp., New York. p. 89.

BROKAW, C. J., and R. JOSSLIN. 1973. Maintenance of constant wave parameters by sperm flagella at reduced frequencies of beat. *J. Exp. Biol.* **59**:617.

BROKAW, C. J.. and D. RINTALA. 1975. Computer simulation of flagellar movement. III. Models incorporating cross-bridge kinetics. *J. Mechanochem. Cell Motility* **3**:77.

BROKAW, C. J., and T. F. SIMONICK. 1976. CO_2 regulation of the amplitude of flagellar bending. *In* Cell Motility. R. Goldman, T. Pollard, and J. Rosenbaum, editors. Cold Spring Harbor Laboratory, New York. In press.

GIBBONS, B. H., and I. R. GIBBONS. 1972. Flagellar movement and adenosine triphosphatase activity in sea urchin sperm extracted with Triton X-100. *J. Cell Biol.* **54**:75.

GIBBONS, B. H., and I. R. GIBBONS. 1974. Properties of flagellar "rigor waves" formed by abrupt removal of adenosine triphosphate from actively swimming sea urchin sperm. *J. Cell Biol.* **63**:970.

GOLDSTEIN, S. F. 1976. Form of developing bends in reactivated sperm flagella. *J. Exp. Biol.* **64**:173.

JEWELL, B. R., and J. C. RUEGG. 1966. Oscillatory contraction of insect fibrillar muscle after glycerol extraction. *Proc. R. Soc. Lond. B. Biol. Sci.* **164**:428.

JULIAN, F. J. 1969. Activation in a skeletal muscle contraction model with a modification for insect fibrillar muscle. *Biophys. J.* **9**:547.

PRINGLE, J. W. S. 1967. The contractile mechanism of insect fibrillar muscle. *Prog. Biophys. Mol. Biol.* **17**:1.

THORSON, J., and D. C. S. WHITE. 1969. Distributed representation for actin-myosin interaction in the oscillatory contraction of muscle. *Biophys. J.* **9**:360.

TREGEAR, R. T. 1975. The biophysics of fibrillar flight muscle. *In* Insect Muscle. P. N. R. Usherwood, editor. Academic Press, London. p. 357.